Performance Enhancement via Incorporation of ZnO Nanolayers in Energetic Al/CuO Multilayers

Lorena Marín, Yuzhi Gao, Maxime Vallet, Iman Abdallah, Bénédicte Warot-Fonrose, Christophe Tenailleau, Antonio T. Lucero, Jiyoung Kim, Alain Estève, Yves J. Chabal, et al.

Performance Enhancement via Incorporation of ZnO Nanolayers in Energetic Al/CuO Multilayers

Lorena Marín,[†,⊥] Yuzhi Gao,[†,§] Maxime Vallet,[‡] Iman Abdallah,[†] Bénédicte Warot-Fonrose,[‡] Christophe Tenailleau,[∥] Antonio T. Lucero,[§] Jiyoung Kim,[§] Alain Esteve,[†] Yves J. Chabal,[§] and Carole Rossi*[,†]

[†]LAAS-CNRS, University of Toulouse, 7 Avenue du colonel Roche, 31077 Toulouse, France

[‡]CEMES-CNRS, University of Toulouse, 29 rue Jeanne Marvig, 31055 Toulouse, France

[§]Department of Materials Science and Engineering, The University of Texas at Dallas, Richardson, Texas 75080, United States

[∥]CIRIMAT-CNRS, 118 Route de Narbonne, F-31062 Toulouse Cedex 9, France

Supporting Information

ABSTRACT: Al/CuO energetic structure are attractive materials due to their high thermal output and propensity to produce gas. They are widely used to bond components or as next generation of MEMS igniters. In such systems, the reaction process is largely dominated by the outward migration of oxygen atoms from the CuO matrix toward the aluminum layers, and many recent studies have already demonstrated that the interfacial nanolayer between the two reactive layers plays a major role in the material properties. Here we demonstrate that the ALD deposition of a thin ZnO layer on the CuO prior to Al deposition (by sputtering) leads to a substantial increase in the efficiency of the overall reaction. The CuO/ZnO/Al foils generate 98% of their theoretical enthalpy within a single reaction at 900 °C, whereas conventional ZnO-free CuO/Al foils produce only 78% of their theoretical enthalpy, distributed over two distinct reaction steps at 550 °C and 850 °C. Combining high-resolution transmission electron microscopy, X-ray diffraction, and differential scanning calorimetry, we characterized the successive formation of a thin zinc aluminate ($ZnAl_2O_4$) and zinc oxide interfacial layers, which act as an effective barrier layer against oxygen diffusion at low temperature.

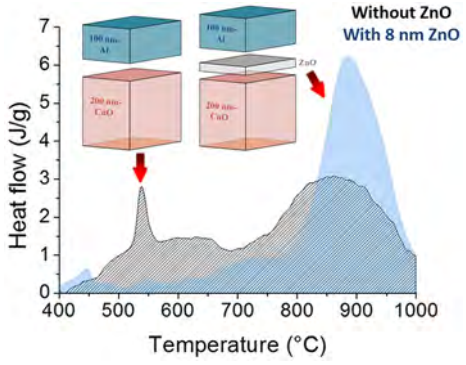

INTRODUCTION

Metal-based energetic structures are the only attractive sources of energy that can be stored for years and yet capable of delivering very quick on-demand bursts of energy in the form of heat and/or pressure. Among the large variety of energetic compounds, thermite nanocomposites, based on exothermic thermite reactions,[1] have attracted great attention over the last two decades.[2] Different types of reactive nanocomposites have been synthesized, such as mixed nanopowders (also called metastable intermolecular composites),[3−6] porous nanocomposites produced by sol−gel synthesis,[7] dense nanocomposites via arrested reactive milling,[8,9] powders deposited by electrophoresis[6,18] and, more recently, 3D printed thick films with tunable fuel and oxidizer nanoarchitectures.[10] Another method is to sputter deposit alternating layers of metal fuel and oxide to form nanolaminate films or foils, also known as reactive multilayers[11−17]

This latter category of materials is very promising and interesting for on-chip integration for several reasons. The reactants are simply vapor-deposited as nanometer-thick layers on top of each other in a repeating sequence, which ultimately produces a thick and sufficiently energetic material without the assembly or production of dangerous products. Additionally, it is easy to control the thickness of each reactant and the number of layers to tune the reaction kinetics and the energy delivered.[15−17] Nanolaminates are capable of long-term chemical energy storage and amenable to integration with microelectronic or MEMS fabrication processes. The Al/CuO nanolaminate is a leading material due to its high thermal output and propensity to produce gas for applications, such as in microinitiators,[20,21] MEMS heat sources,[18,19] or exploding foil initiators.[22] As published previously,[23] the nanolaminate reaction process is largely dominated by the outward migration of oxygen atoms from the CuO toward the aluminum layers. One challenge associated with the integration of such Al/CuO nanolaminates for tangible practical applications lies in the mastering of interface interactions to produce and accurately control the expected performances. During sputter deposition, the polycrystalline Al and CuO layers intermix to form an amorphous interface.[24] In a subsequent step, these interfaces, under heating, allow fast transport of O from CuO to Al. For individual layers with thicknesses below 200 nm, the ratio

DOI: 10.1021/acs.langmuir.7b02964

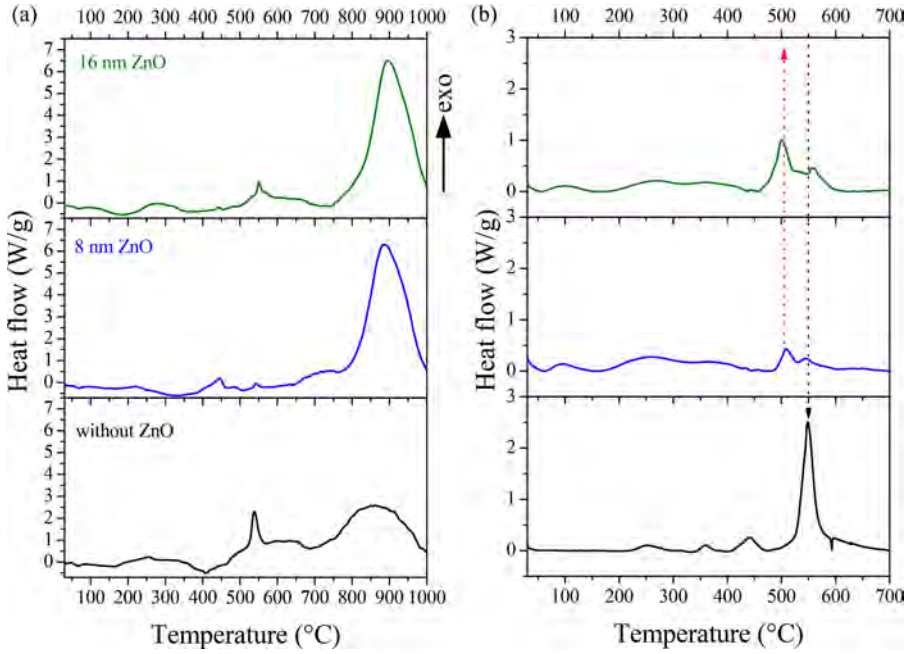

Figure 1. DSC traces showing the exotherms and endotherms upon heating to 1000 °C at 10 °C/min (a) from ambient temperature to 1000 °C and (b) from ambient temperature to 700 °C.

between the reactive layers (Al and CuO) and the interfacial layers is such that the interface zone becomes dominant, governing the properties of the overall reactive materials. For example, depositing 10 nm of Cu on top of Al prior to the deposition of CuO has been shown to improve the overall reactivity of Al/CuO nanolaminates because it prevents the formation of interfacial alumina and leads to the formation of Al_2Cu crystals at low temperature (<300 °C).[25,26] The beneficial role of Cu in Al/Cu_2O nanolaminates has also been demonstrated by Kinsey et al.[27] Interlayers of Cu (25 to 100 nm in thickness) sputtered in Al/Cu_2O reactive multilayers reduce the reaction temperature and thus suppress the metal vaporization.

Here we specifically address the issue of interface formation during Al sputtering onto the CuO layer, which is the main source of vulnerability in sputter-deposited Al/CuO multilayers, causing uncontrollable reactivity, unreliability in performance, and potential aging problems. Naturally, during sputtering, the top surface of CuO is spontaneously reduced upon Al atom deposition, producing a rough and inhomogeneous interfacial layer along the rough CuO surface region that is composed of a mixture of Al, Cu, and O and likely has a high density of defects.[24]

Our goal here is to produce a *high-quality interface* between reactive CuO and Al layers by depositing a thin ZnO layer on top of CuO prior to Al deposition to prevent the reduction of the CuO film when the Al atoms react with the CuO surface. ZnO is selected because (1) it is a stable oxide characterized by a wide bandgap (3.37 eV) and a high exciton bond energy (60 meV), therefore providing better control with lower chemical reactivity when exposed to Al, (2) it is much less reactive than CuO in contact with Al,[28] therefore minimizing Al oxidation during the sputtering process, and (3) it is one of the most technologically relevant oxides (i.e., commonly used) for a vast number of applications and can be deposited via pulsed laser deposition,[29] sputtering,[30] and atomic layer deposition (ALD).[31] For this fundamental study, ALD is selected to obtain conformal and continuous coverage over the intrinsically rough CuO film, thus allowing a more systematic atomic-level investigation. However, ZnO can also be sputter-deposited as are both Al and CuO layers within the nanolaminate fabrication process.

Two thicknesses were selected for the interfacial ZnO layer, 8 and 16 nm. The thermal properties of the CuO/Al bilayer systems, with and without interfacial ZnO layers, were analyzed and compared. For each sample, scanning transmission electron microscopy (STEM), electron energy-loss spectroscopy (EELS), transmission electron microscopy (TEM), and X-ray diffraction (XRD) were performed to characterize the interfaces of as-deposited samples and their evolution after quenching at 700 °C. The results demonstrate that adding a very thin ZnO layer prior to the Al sputtering leads to the formation, at relative low temperature, of a stable $ZnAl_2O_4$ interfacial layer, and at moderate temperature, to the crystallization of ZnO, both acting as effective barrier layers to oxygen migration. This new method provides the foundation for stabilizing Al/CuO nanolaminates, thus controlling their aging. It can be generalized to any Al-based thermite multilayer, opening this new class of material to many applications, such as welding, microthermal sources, microactuators, in situ welding and soldering, local enhancement of chemical reactions, nanosterilization, and controlled cell apoptosis and ignition.

EXPERIMENTAL METHODS

Materials and Deposition Processes. CuO and Al layers were produced via DC magnetron sputtering on a silicon wafer using aluminum and copper targets from Neeco (Vanves, France) with a purity of 99.999%. The conditions for sputtering were previously reported.[25] For the CuO/ZnO/Al foils, a ZnO film was deposited on CuO via ALD using a Savannah-100 ALD reactor (Cambridge NanoTech) at 130 °C, using diethylzinc (DEZ) and water vapor precursors as sources for zinc and oxygen atoms. The process pressure was ~50 mTorr, and the N_2 purging gas flow rate was 20 sccm, with respective pulse times of 0.03 s for diethylzinc, 0.1 s for water, and 20 s N_2 purge for a total of 44 and 88 cycles to obtain 8 and 16 nm

Table 1. Heat Released during the First Exotherm (530−570 °C), the Second Exotherm (700−1000 °C), and the Full Scans (530−1000 °C)

sample	peak 1 [J/g] (530−570 °C)	peak 2 [J/g] (700−1000 °C)	total (peak 1 + peak 2) [J/g] (530−1000 °C)
reference	403 ± 15	2676	3079
8 nm of ZnO	–	3831	3831
16 nm of ZnO	–	3751	3751

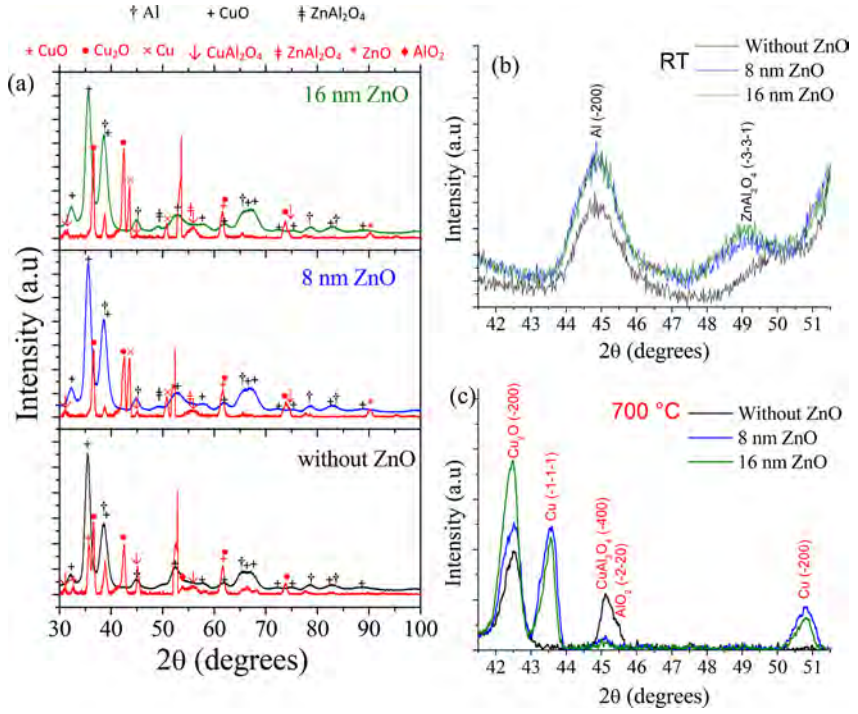

Figure 2. X-ray diffractograms of as-deposited foils (black color) and after quenching at 700 °C (red color). (a) Bottom, middle, and top diagrams correspond to CuO/Al, CuO/ZnO/Al (8 nm of ZnO), and CuO/ZnO/Al (16 nm of ZnO), respectively. (b) Zoom between 42° and 60° for as-deposited foils and (c) for the same foils quenched at 700 °C. Compounds written in red below the XRD diagrams correspond to the compounds detected after annealing at 700 °C (RT: room temperature).

thicknesses, respectively. The XRD spectra of the as-deposited ZnO films (see Supporting Information Figure S1) show that, at room temperature, it is crystalline when deposited on Si substrate, whereas it is amorphous when deposited on CuO. Prior to deposition, the initial oxidized surfaces of the silicon wafers were cleaned via a 5 min plasma treatment to remove impurities and contaminants and increase the OH coverage needed for photoresist spin coating. A layer of photoresist (NLOF-5 μm) was then spin coated and baked at 110 °C for 90 s prior to CuO sputter deposition. That photoresist was later dissolved in acetone to release the nanolaminates.

Two types of samples were prepared: (i) CuO/Al bilayer foils with a natural interface and (ii) CuO/ZnO/Al foils with ZnO thicknesses of 8 and 16 nm. In all samples, the thicknesses of the CuO and Al layers were fixed at 200 and 100 nm, respectively, to optimize a stoichiometric O/Al ratio.

Thermal Analysis. The exothermic reactions of the foils were characterized via DSC using a Mettler-Toledo device with a HSS8 sensor in the temperature range of 30 °C to 700 °C and also a TGA-DTA SETARAM device (type S thermocouple) in the temperature range of 30 °C to 1000 °C. All thermal analyses were performed under a constant heating rate (10 °C/min) in an Ar atmosphere purified by passing through an oxygen trap (Supelco) that provided a purity of >99.999%. The foils, prepared and released from their substrates as described in the previous section, were placed into a 150-μL platinum pan. After the first heating cycle, the sample was cooled to room temperature and then heated again at the same heating rate. This second analysis was used to correct the baseline, assuming that the bulk heat capacity of the sample did not change between the first and the second heating runs.

Structural and Chemical Characterization. Crystalline phases were detected using grazing incidence X-ray diffraction (Bruker D8 Discover system) with a Cu Kα radiation as the source. The grazing angle was fixed at 1°, and the 2θ collection angle varied from 30° to 100° with a 0.02° step and a dwell time of 1 s per point in all cases. The XRD experiments were performed on as-deposited (just after sputtering) and on samples annealed at 700 °C (just before the main reaction peak) to detect the formation of different phases and their dependence on the interfacial ZnO thickness. Cross-sectional TEM experiments were performed on samples prepared using a focused-ion beam (FIB) in the FEI Helios Nanolab. HAADF-STEM was performed using a JEOL cold-FEG JEM-ARM200F operated at 200 kV and equipped with a probe Cs corrector that has a maximum spatial resolution of 0.078 nm. The EELS experiments were performed using a GIF Quantum ER, and the EDX spectra were recorded with a JEOL CENTURIO SDD detector.

RESULTS

Thermal Properties. Figure 1(a) shows the DSC thermal diagrams of the CuO/Al foils with and without the ZnO interfacial layer. The CuO/Al samples are characterized by two major peaks, as previously mentioned in several papers. The first one occurs prior to the melting of Al at 550 °C (Figure 1(b)) and is attributed to the reduction of CuO into Cu_2O that consequently leads to Al oxidation, limited to the interfacial

region; this first process yields less than one-third of the total reservoir of heat in the CuO/Al foils (Table 1). Note that the contribution of the first exothermic peak relative to the total heat of reaction greatly depends on Al and CuO layer thicknesses. The second major exotherm occurs at 850 °C and may correspond to the main thermite reaction when Cu_2O releases its oxygen to produce a pure copper material. The migration of the released oxygen toward the pure Al layers gives rise to oxidation reactions and the formation of an alumina phase.

In contrast, the DSC traces clearly indicate that the Al+CuO reaction occurs in only one main step at approximately ~900 °C for all the CuO/ZnO/Al samples, as the total contribution of the broad and small exotherms around 500 °C (see Figure 1(b) top and middle traces) only amounts ~0.3% of the total heat. We hypothesized that these first weak and shallow peaks that were observed in the CuO/ZnO/Al foils do not correspond to Al oxidation close to the interface but may instead correspond to the formation and crystallization of ZnO itself, as reported previously[33] and discussed in the following sections. The main reaction exotherm is much more pronounced (Figure 1(a) top and middle traces) when a thin layer of ZnO replaces the *natural* interface, indicating that the Al reservoir is not consumed by the oxidation of Al near the interface at low temperature producing amorphous alumina (not seen in XRD spectra of Figure 2).

The heat released during the DSC scans, calculated by integrating the exothermic peaks over time in the ranges of 530 °C to 570 °C and 700 °C to 1000 °C and normalizing with respect to the foil mass, is reported in Table 1 for the three different foils. The heat release calculation highly depends on the DSC curves baseline determination; therefore, the values in J/g reported in Table 1 are indicative and interesting for the foils comparison.

The total heat of reaction obtained for the CuO/ZnO/Al foils is 1.2 times greater than that of the CuO/Al foils. Adding a thin layer of ZnO between the CuO and Al layer preserves the integrity of the deposited Al layer possibly by reducing oxygen migration through Zn-based barrier layers; consequently, 98% of the theoretical Al/CuO enthalpy (3.9 kJ/g) can be released at the end of the scan in a single step. Assuming a crystalline ZnO layer, the 8 nm- and 16 nm-thick ZnO layers contribute only ~3.3% and 6.6% additional oxygen, respectively, into the bilayer, which cannot be the reason for the ~20% increase in the heat of the reaction.

XRD Analysis. X-ray diffraction patterns obtained on both freshly sputtered foils (black) and foils quenched at 700 °C (just before the main reaction peak) (red) are shown in Figure 2(a).

After Deposition by Sputtering. CuO (+) and Al (†) clearly constitute the main phases. The peak at ~38.9° includes contributions from Al (111) and CuO (111). None of the alumina peaks are observed in the XRD patterns. At this stage, there is no detectable peak associated with ZnO in Al/ZnO/CuO, while a zinc aluminate ($ZnAl_2O_4$) phase is clearly identified at 49.062° (Figure 2(b)). Note that observations (see XRD diagram in Supporting Information Figure S1(b)) suggest that ZnO deposited on CuO at room temperature is amorphous and becomes crystalline (possibly epitaxial) at 700 °C.

After Annealing. Annealing at 700 °C induces clear changes in the diffraction patterns. Additional peaks associated with Cu_2O (at 73.863°) are observed, consistent with the expected oxygen loss of CuO observed for all samples. The comparison between the diffractograms of zinc oxide-free foils and those containing different ZnO interfacial layers reveals the following. In ZnO-free foils, the $CuAl_2O_4$ peak intensity clearly increases (Figure 2(c)) whereas it does not appear in foils with a ZnO interfacial layer. This indicates that, in the ZnO-free foils, the amorphous Al_2O_3 produced by the oxidation of Al close to the interface (onset at 500 °C, i.e., the first exotherm of the DSC trace, Figure 1(b) bottom diagram) may be transformed into γ-Al_2O_3 which can immediately react with CuO to form $CuAl_2O_4$, a ternary oxide that contributes to stop any further reaction between Al and CuO below 900 °C, possibly because of its high density. In foils with ZnO interfacial layers, the spontaneous formation of $ZnAl_2O_4$ at low temperature stabilizes the overall nanolaminate until high temperature reaction (850 °C), playing a similar role $CuAl_2O_4$ in the ZnO-free foils.

Additionally in CuO/ZnO/Al stacks, the diffractograms show the presence of pure copper in addition to Al, CuO, and Cu_2O species. The presence of metallic Cu (×) and ZnO (*) was not detected for the ZnO-free foils. This suggests the occurrence of new multiple reactions due to the initial reduction of ZnO via Al sputtering. Then Zn metal may react with the near surface of CuO to produce ZnO and Cu.

TEM analysis was performed on the CuO/ZnO/Al stacks with only an 8 nm-thick ZnO layer, immediately after sputter deposition of Al to examine the microstructure, thickness, and chemical composition of the interfacial layer that acts as a good barrier layer. As expected, the cross-sectional pictures (Figure 3) show that the thin interfacial layer conforms to the highly

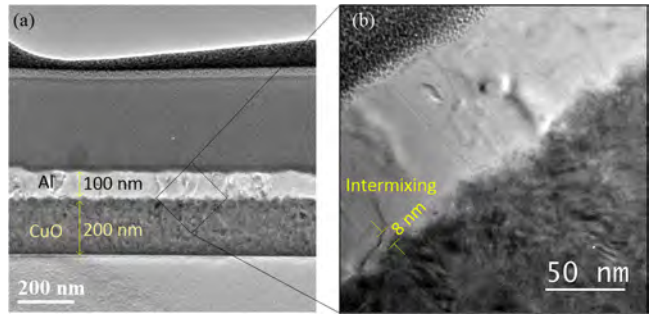

Figure 3. Bright-field TEM cross-sections of CuO/ZnO/Al deposited on silicon with a ZnO thickness of 8 nm. (a) Intermediate and (b) high magnification.

textured CuO surface and that Al and CuO layers are both polycrystalline. A more magnified TEM image (Figure 3(b)) shows that there is a thin interfacial layer between Al and ZnO, resulting from intermixing.

EELS measurements were used to evaluate the chemical composition of this interfacial intermixing region by considering two energy ranges simultaneously: 700−1723.5 eV to detect the metallic edge (copper, zinc, and aluminum) and 400−1423.5 eV to detect oxygen atoms, and the spectral shape inferred changes in the environment (e.g., surrounding metallic atoms). The results are reported in Figure 4 and show the chemical composition evolution across ~40 nm of the interface from the Al to the CuO layer. Three regions are distinct (Figure 4(a)): a first aluminum-rich region, a second region (~15 nm thick) where aluminum coexist with Cu and Zn atoms, and a third region (~10 nm thick) where only Cu and Zn are detected. For each region, two spectra are recorded, separated by 5 nm, to analyze the coexistence of Al, Cu, and Zn

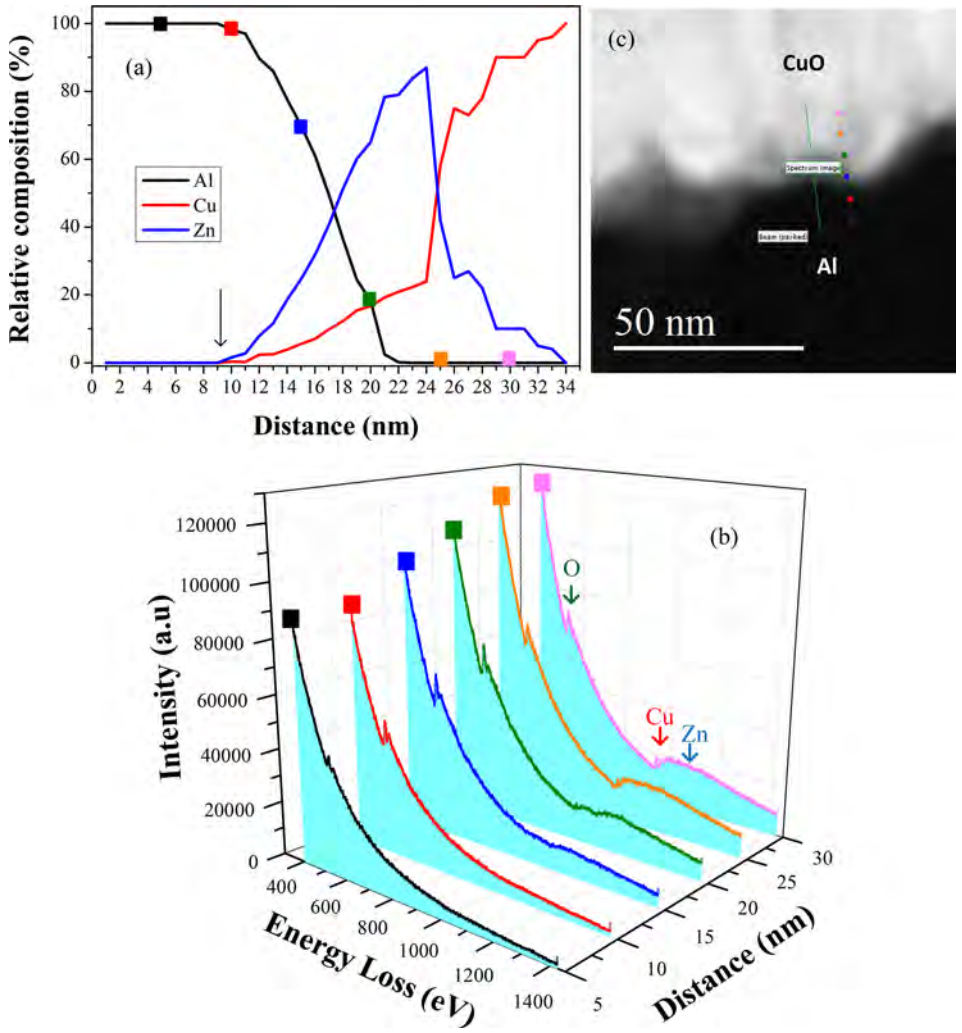

Figure 4. (a) Chemical composition (presence of Al, Cu, and Zn) as a function of position in CuO/ZnO/Al stacks with 8 nm of ZnO. (b) Actual EELS spectra showing both the Cu and Zn and oxygen as a function of position. (c) HAADF-STEM image of the analyzed area using color-coded squares to correlate to the spectra shown in b.

with oxygen atoms (Figure 4(b)). The exact positions of the measurements are marked with color-coded squares in the STEM image shown in Figure 4(c).

The first region (black and red squares) contains aluminum and oxygen atoms because the edge of oxygen has two well-defined peaks and the signature of the oxygen peak shows it is an aluminum oxide as detailed in Supporting Information Figure S2). The second region contains Al, O, Zn, which is consistent with the XRD observation of a $ZnAl_2O_4$ phase and additional Cu (green spectra) in a more limited quantity. In the third region, when the neighboring atoms are copper instead of aluminum, the edge of the oxygen is modified (see Supporting Information Figure S2). One small signal from metallic Zn is also detected in the same spectrum (orange spectrum). Note that in the XRD measurements, a ZnO interface could not be clearly identified after Al deposition, which indicates a possible formation of $ZnAl_2O_4$ when Al is sputter deposited on the interfacial ZnO layer.

Beyond this interfacial region, the presence of the aluminum edge decreases compared to the spectral features associated with Zn and Cu. In addition, the atoms with which it was bound affected the oxygen edge shape. Through the interface, we identified Al+O+Zn with CuO and CuO with Zn. From this composition analysis alone, we found some extended overlap between the different species, which makes it difficult to precisely determine the nature of the interfacial domain. This is due to the rough nature of the interface along which the scan was performed. However, the overall analysis is totally consistent with the structural investigation.

DISCUSSION

In this work, the thickness of each CuO and Al film was kept constant, ensuring the same quantity and quality for the reactant layers. XRD measurements indicated that the foils contain Al and CuO layers, and STEM images confirmed that their respective thicknesses were 100 and 200 nm. Nanolaminate foils with 8 nm- and 16 nm-thick ZnO interfacial layers yield 98% of the theoretical enthalpy in a single step at ~900 °C, whereas nanolaminate foils without ZnO interfacial layers (i.e., original interfaces) deliver only 74% of their theoretical enthalpy spread over two distinct exotherms at 550 °C and 850 °C. The three central mechanisms that control their overall performance are as follows and discussed below: (1) a thin $ZnAl_2O_4$ spinel phase seems to be spontaneously formed upon sputter deposition of Al on ZnO at room temperature, a phase that usually requires much higher

temperature (>800 °C) to be synthesized via a solid-state reaction of zinc and aluminum oxides;[34,35] (2) this $ZnAl_2O_4$ layer prevents Al oxidation during Al sputter deposition at temperatures below 700 °C; (3) there is interdiffusion of metallic Zn into CuO upon heating to form ZnO and metallic Cu.

.

Formation of a $ZnAl_2O_4$ Crystalline Phase upon Sputter Deposition of Al on ZnO and Release of Metallic Zn Atoms. As detected by XRD, sputter deposition of Al on ZnO thin films leads to the formation of thin $ZnAl_2O_4$ layer with predominantly (331) orientation. To confirm this scenario, an additional foil was prepared, in which 2 nm of Al_2O_3 was deposited via ALD on ZnO prior to sputter deposition of Al. In this foil (CuO-200 nm/ZnO-8 nm/Al_2O_3-2 nm/Al-100 nm), no $ZnAl_2O_4$ was detected via XRD (see Supporting Information Figure S3). Therefore, a thin conformal Al_2O_3 layer is enough to prevent ZnO and Al intermixing that would lead to $ZnAl_2O_4$ formation. A recent experimental study of the basic mechanisms of Al interaction with ZnO surfaces[32] has shown that Al reduces ZnO by forming Al_2O_3, releasing metallic Zn to the surface, eventually leading to the formation of $ZnAl_2O_4$. This work further shows that the deposition of a thin (~2 nm) Al_2O_3 layer on ZnO prior to Al deposition effectively prevents Al penetration into ZnO and associated Zn release, thus requiring higher temperatures to oxidize Al. Additionally, the observation of $ZnAl_2O_4$ is in good agreement with a previous study of Ohmic and Schottky Al contacts on ZnO,[36] which showed that at room temperature some oxygen atoms diffuse out from the ZnO to the Al metal layer and Al atoms diffuse into the ZnO. The chemical evolution of ZnO in the surface region is possible at room temperature as a result of the extensive and highly exothermic reaction between Al and O in the ZnO layer. As a $ZnAl_2O_4$ phase is formed upon the arrival of Al on ZnO, oxygen vacancies produced in the ZnO layer may promote the formation of metallic Zn: $2Al + 4\ ZnO \rightarrow ZnAl_2O_4 + 3\ Zn$.

Interdiffusion of Free Zn Atoms into CuO To Form ZnO and Metallic Cu. Two observations presented above support the mechanism where metallic Zn atoms generated from the reaction of Al with ZnO can locally react with copper oxide to form ZnO and metallic Cu. First, Cu metal was detected in both the X-ray diffractograms (Figure 2(c)) and from EELS analysis (Figure 4). Second, enthalpy considerations also rationalize the formation of ZnO. The enthalpies generated during the first exotherms (Figure 1(b), top and middle diagrams), extracted from the two exotherms at 450 to 550 °C and normalized to the foil masses, are 340.93 and 674.37 mJ for foils with 8 and 16 nm of ZnO, respectively. The fact that the calculated enthalpies for the 16 nm-thick foil is twice that of the 8 nm-thick foil of ZnO supports the proposed reaction Zn + CuO (with enthalpy = 1.33 kJ/g), where Zn was initially produced by the reaction of ZnO with Al. We deduce a mass of 2.6×10^{-4} and 5.0×10^{-4} g of ZnO associated with the reaction.

Protective Effect of $ZnAl_2O_4$ against Al Oxidation below Its Melting Point. The $ZnAl_2O_4$ layer appears to be an effective barrier layer because no interaction between Al and CuO is possible below the main reaction peak at 900 °C. Complementary experiments were conducted (see Supporting Information S4) to experimentally support this conclusion. CuO/Al and CuO/ZnO/Al foils were prepared, as described in Experimental Methods, after being left at room temperature for 250 days, and XRD analyses were performed to determine the phase evolution during this time. Without ZnO at the interface, a Cu_2O phase appeared after 250 days of aging at room temperature, whereas it did not appear when a ZnO interfacial layer was present. This last experiment clearly confirmed the good protective effect of $ZnAl_2O_4$ against the diffusion of oxygen from the CuO to Al layer.

CONCLUSION

This work shows that the deposition of a thin ZnO layer at the CuO/Al interface results in a modification of the Al+CuO energetic properties. With a ZnO interfacial layer, Al/CuO foils generate 98% of their theoretical enthalpy within a single reaction step at 900 °C, whereas ZnO-free CuO/Al foils produce less amount of heat distributed over two distinct reaction steps at 550 °C and 850 °C.

This difference is due to multiple and complex processes (alloying, phase transformations) taking place at both ZnO interfaces (e.g., with CuO and Al) and upon annealing up to 700 °C. First of all, during Al deposition, metallic zinc is produced from ZnO reduction, with the concomitant formation of $ZnAl_2O_4$. In a second step, at higher temperature, between 450 °C and 550 °C, liberated zinc atoms reduce copper oxide, leading to the formation of crystalline ZnO and pure copper. All these reaction steps and formation of Zn-based derivatives are reducing oxygen diffusion, preserving the overall aluminum reservoir from oxidation at low temperature. For what concerns ZnO-free foils, copper oxide may interact with Al_2O_3 (amorphous and then γ alumina) produced between 500 °C and 570 °C (first exotherm) to create $CuAl_2O_4$ ternary oxide layer that contributes in blocking the solid–solid interaction between both reactive compounds before Al melting. The derived mechanistic understanding of this new method for stabilizing and controlling the thermal and chemical properties of Al/CuO nanolaminates, notably their stability, will provide a basis for generalizing it to any Al-based thermite multilayer.

ASSOCIATED CONTENT

Supporting Information

The Supporting Information is available free of charge on the ACS Publications website at DOI: 10.1021/acs.langmuir.7b02964.

EELS spectra and X-ray patterns (PDF)

AUTHOR INFORMATION

Corresponding Author

*E-mail: carole.rossi@laas.fr.

ORCID

Jiyoung Kim: 0000-0003-2781-5149

Yves J. Chabal: 0000-0002-6435-0347

Carole Rossi: 0000-0003-3864-7574

Present Address

[⊥]Departamento de Física, Grupo de Películas Delgadas, Universidad del Valle, A.A 25360 Cali, Colombia.

Author Contributions

The manuscript was written with contributions from all authors. All authors have approved the final version of the manuscript.

Notes

The authors declare no competing financial interest.

■ ACKNOWLEDGMENTS

The authors thank the French Technological Network, RENATECH, for partially funding the sputter deposition equipment and the French CNRS for financial support of the METSA network (FR3507). We also thank Pierre Alphonse from CIRIMAT for assistance with the DSC experiments, Alexandre Arnoult from LAAS for assistance with the XRD measurements, and Cécile Garcia from CEMES and Teresa Hungria-Hernandez from Centre de Microcaractérisation Raimond Castaing (UMS3623) for assistance with the TEM experiments. This research was supported by the CNRS (LIA-ATLAB), the Université Fédérale de Toulouse (MUSE) and ANR grant IMPYACT (132497-LabCom2015).

■ REFERENCES

(1) Fischer, S.; Grubelich, M. A Survey of Combustible Metals, Thermites, and Intermetallics for Pyrotechnic Applications. In *32nd Joint Propulsion Conference and Exhibit*; American Institute of Aeronautics and Astronautics: Reston, VA, 1996.

(2) Rossi, C. Innovating in Energetic Materials from the Bottom. *Propellants, Explos., Pyrotech.* **2017**, *42* (3), 235−236.

(3) Bockmon, B. S.; Pantoya, M. L.; Son, S. F.; Asay, B. W.; Mang, J. T. Combustion Velocities and Propagation Mechanisms of Metastable Interstitial Composites. *J. Appl. Phys.* **2005**, *98* (6), 64903.

(4) Weismiller, M. R.; Malchi, J. Y.; Lee, J. G.; Yetter, R. A.; Foley, T. J. Effects of Fuel and Oxidizer Particle Dimensions on the Propagation of Aluminum Containing Thermites. *Proc. Combust. Inst.* **2011**, *33* (2), 1989−1996.

(5) Puszynski, J. A. Processing and Characterization of Aluminum-Based Nanothermites. *J. Therm. Anal. Calorim.* **2009**, *96* (3), 677−685.

(6) Sullivan, K. T.; Worsley, M. A.; Kuntz, J. D.; Gash, A. E. Electrophoretic Deposition of Binary Energetic Composites. *Combust. Flame* **2012**, *159* (6), 2210−2218.

(7) Tillotson, T.; Gash, A.; Simpson, R.; Hrubesh, L.; Satcher, J.; Poco, J. Nanostructured Energetic Materials Using Sol−gel Methodologies. *J. Non-Cryst. Solids* **2001**, *285* (1−3), 338−345.

(8) Stamatis, D.; Jiang, Z.; Hoffmann, V. K.; Schoenitz, M.; Dreizin, E. L. Fully Dense, Aluminum-Rich Al-CuO Nanocomposite Powders for Energetic Formulations. *Combust. Sci. Technol.* **2008**, *181* (1), 97−116.

(9) Stamatis, D.; Zhu, X.; Schoenitz, M.; Dreizin, E. L.; Redner, P. Consolidation and Mechanical Properties of Reactive Nanocomposite Powders. *Powder Technol.* **2011**, *208* (3), 637−642.

(10) Sullivan, K. T.; Zhu, C.; Duoss, E. B.; Gash, A. E.; Kolesky, D. B.; Kuntz, J. D.; Lewis, J. A.; Spadaccini, C. M. Controlling Material Reactivity Using Architecture. *Adv. Mater.* **2016**, *28* (10), 1934−1939.

(11) Adams, D. P. Reactive Multilayers Fabricated by Vapor Deposition: A Critical Review. *Thin Solid Films* **2015**, *576*, 98−128.

(12) Blobaum, K. J.; Reiss, M. E.; Plitzko, J. M.; Weihs, T. P. Deposition and Characterization of a Self-Propagating CuOx/Al Thermite Reaction in a Multilayer Foil Geometry. *J. Appl. Phys.* **2003**, *94* (5), 2915−2922.

(13) Petrantoni, M.; Rossi, C.; Salvagnac, L.; Conédéra, V.; Estève, A.; Tenailleau, C.; Alphonse, P.; Chabal, Y. J. Multilayered Al/CuO Thermite Formation by Reactive Magnetron Sputtering: Nano versus Micro. *J. Appl. Phys.* **2010**, *108* (8), 84323 10.1063/1.3498821.

(14) Amini-Manesh, N.; Basu, S.; Kumar, R. Modeling of a Reacting Nanofilm on a Composite Substrate. *Energy* **2011**, *36* (3), 1688−1697.

(15) Bahrami, M.; Taton, G.; Conédéra, V.; Salvagnac, L.; Tenailleau, C.; Alphonse, P.; Rossi, C. Magnetron Sputtered Al-CuO Nanolaminates: Effect of Stoichiometry and Layers Thickness on Energy Release and Burning Rate. *Propellants, Explos., Pyrotech.* **2014**, *39* (3), 365−373.

(16) Egan, G. C.; Mily, E. J.; Maria, J.-P.; Zachariah, M. R. Probing the Reaction Dynamics of Thermite Nanolaminates. *J. Phys. Chem. C* **2015**, *119* (35), 20401−20408.

(17) Manesh, N. A.; Basu, S.; Kumar, R. Experimental Flame Speed in Multi-Layered Nano-Energetic Materials. *Combust. Flame* **2010**, *157* (3), 476−480.

(18) Zhou, X.; Ke, X.; Jiang, W. Aluminum/copper Oxide Nanostructured Energetic Materials Prepared by Solution Chemistry and Electrophoretic Deposition. *RSC Adv.* **2016**, *6* (96), 93863−93866.

(19) Zhou, X.; Wang, Y.; Cheng, Z.; Ke, X.; Jiang, W. Facile Preparation and Energetic Characteristics of Core-Shell Al/CuO Metastable Intermolecular Composite Thin Film on a Silicon Substrate. *Chem. Eng. J.* **2017**, *328*, 585−590.

(20) Taton, G.; Lagrange, D.; Conedera, V.; Renaud, L.; Rossi, C. Micro-Chip Initiator Realized by Integrating Al/CuO Multilayer Nanothermite on Polymeric Membrane. *J. Micromech. Microeng.* **2013**, *23* (10), 105009.

(21) Zhu, P.; Shen, R.; Ye, Y.; Zhou, X.; Hu, Y. Energetic Igniters Realized by Integrating Al/CuO Reactive Multilayer Films with Cr Films. *J. Appl. Phys.* **2011**, *110* (7), 74513.

(22) Zhou, X.; Shen, R.; Ye, Y.; Zhu, P.; Hu, Y.; Wu, L. Influence of Al/CuO Reactive Multilayer Films Additives on Exploding Foil Initiator. *J. Appl. Phys.* **2011**, *110* (9), 94505.

(23) Blobaum, K. J.; Wagner, A. J.; Plitzko, J. M.; Van Heerden, D.; Fairbrother, D. H.; Weihs, T. P. Investigating the Reaction Path and Growth Kinetics in CuOx/Al Multilayer Foils. *J. Appl. Phys.* **2003**, *94* (5), 2923−2929.

(24) Kwon, J.; Ducéré, J. M.; Alphonse, P.; Bahrami, M.; Petrantoni, M.; Veyan, J.-F.; Tenailleau, C.; Estève, A.; Rossi, C.; Chabal, Y. J. Interfacial Chemistry in Al/CuO Reactive Nanomaterial and Its Role in Exothermic Reaction. *ACS Appl. Mater. Interfaces* **2013**, *5* (3), 605−613.

(25) Marín, L.; Warot-Fonrose, B.; Estève, A.; Chabal, Y. J.; Alfredo Rodriguez, L.; Rossi, C. Self-Organized Al 2 Cu Nanocrystals at the Interface of Aluminum-Based Reactive Nanolaminates to Lower Reaction Onset Temperature. *ACS Appl. Mater. Interfaces* **2016**, *8* (20), 13104−13113.

(26) Marín, L.; Nanayakkara, C. E.; Veyan, J.-F.; Warot-Fonrose, B.; Joulie, S.; Estève, A.; Tenailleau, C.; Chabal, Y. J.; Rossi, C. Enhancing the Reactivity of Al/CuO Nanolaminates by Cu Incorporation at the Interfaces. *ACS Appl. Mater. Interfaces* **2015**, *7* (22), 11713−11718.

(27) Kinsey, A. H.; Slusarski, K.; Woll, K.; Gibbins, D.; Weihs, T. P. Effect of Dilution on Reaction Properties and Bonds Formed Using Mechanically Processed Dilute Thermite Foils. *J. Mater. Sci.* **2016**, *51* (12), 5738−5749.

(28) Maleki, A.; Panjepour, M.; Niroumand, B.; Meratian, M. Mechanism of Zinc Oxide−aluminum Aluminothermic Reaction. *J. Mater. Sci.* **2010**, *45* (20), 5574−5580.

(29) Tsoutsouva, M. G.; Panagopoulos, C. N.; Papadimitriou, D.; Fasaki, I.; Kompitsas, M. ZnO Thin Films Prepared by Pulsed Laser Deposition. *Mater. Sci. Eng., B* **2011**, *176* (6), 480−483.

(30) Damiani, L. R.; Mansano, R. D. Zinc Oxide Thin Films Deposited by Magnetron Sputtering with Various Oxygen/argon Concentrations. *J. Phys. Conf. Ser.* **2012**, *370*, 12019.

(31) Tynell, T.; Karppinen, M. Atomic Layer Deposition of ZnO: A Review. *Semicond. Sci. Technol.* **2014**, *29* (4), 43001.

(32) Gao, Y.; Marín, L.; Mattson, E. C.; Cure, J.; Nanayakkara, C. E.; Veyan, J. F.; Lucero, A.; Kim, J.; Rossi, C.; Esteve, A.; Chabal, Y. J. Basic Mechanisms of Al Interaction with the ZnO Surface. *J. Phys. Chem. C* **2017**, *121* (23), 12780−12788.

(33) Chen, K. J.; Fang, T. H.; Hung, F. Y.; Ji, L. W.; Chang, S. J.; Young, S. J.; Hsiao, Y. J. The Crystallization and Physical Properties of Al-Doped ZnO Nanoparticles. *Appl. Surf. Sci.* **2008**, *254* (18), 5791−5795.

(34) Hong, W.-S.; De Jonghe, L. C.; Yang, X.; Rahaman, M. N. Reaction Sintering of ZnO-AI 2 O 3. *J. Am. Ceram. Soc.* **1995**, *78* (12), 3217−3224.

(35) Keller, J. T.; Agrawal, D. K.; McKinstry, H. A. Quantitative XRD Studies of ZnAl 2 O 4 (Spinel) Synthesized by Sol-Gel and Powder Methods. *Adv. Ceram. Mater.* **1988**, *3* (4), 420−422.

(36) Kim, H. K.; Seong, T. Y.; Kim, K. K.; Park, S. J.; Yoon, Y. S.; Adesida, I. Mechanism of Nonalloyed Al Ohmic Contacts to N-Type ZnO:Al Epitaxial Layer. *Japanese J. Appl. Physics, Part 1 Regul. Pap. Short Notes Rev. Pap.* **2004**, *43* (3), 976–979.

Supporting Information

Performance enhancement via incorporation of ZnO nanolayers in energetic Al:CuO multilayers

Lorena Marín[†•], Yuzhi Gao[†♦], Maxime Vallet[Ψ], Iman Abdallah[†], Bénédicte Warot-Fonrose[Ψ], Christophe Tenailleau[δ], Antonio T. Lucero[♦], Jiyoung Kim[♦], Alain Esteve[†], Yves J. Chabal[♦], Carole Rossi[†]*

[†] LAAS-CNRS, University of Toulouse, 7 Avenue du colonel Roche, 31077 Toulouse, France

[Ψ] CEMES-CNRS, University of Toulouse, 29 rue Jeanne Marvig, 31055 Toulouse, France

[♦] Department of Materials Science and Engineering, The University of Texas at Dallas, Richardson, Texas 75080, United States

[δ]CIRIMAT-CNRS, 118 Route de Narbonne, F-31062 Toulouse Cedex 9, France

KEYWORDS. ZnO barrier layer, reactive nanolaminates, aluminum copper system, reactive interfaces.

Supporting Information Figure S1. X-ray patterns of 16 nm thick ALD ZnO deposited on Si and CuO (200 nm) measured in a 200 μm x 200 μm region

The XRD spectrum of the ALD ZnO film on silicon substrate, is shown in Figure S1 (a). All the ZnO peaks are labeled by the corresponding crystallographic axes. Therefore, it is evident that the preferred orientation is along (0 0 -2) direction. In addition, there is broad band centered at 56.40° that is assigned to a contribution from the Zn_2SiO_4 phase, suggesting that there is some interaction between the Zn precursor and the underlying Si film during the initial stage of the process leading to a thin composite interface layer. The large width is consistent with a very thin film. On the other hand, there is a sharper contribution at 51.49° from the underlying Si substrate as expected. These observations suggest that ZnO deposited on CuO at room temperature is amorphous.

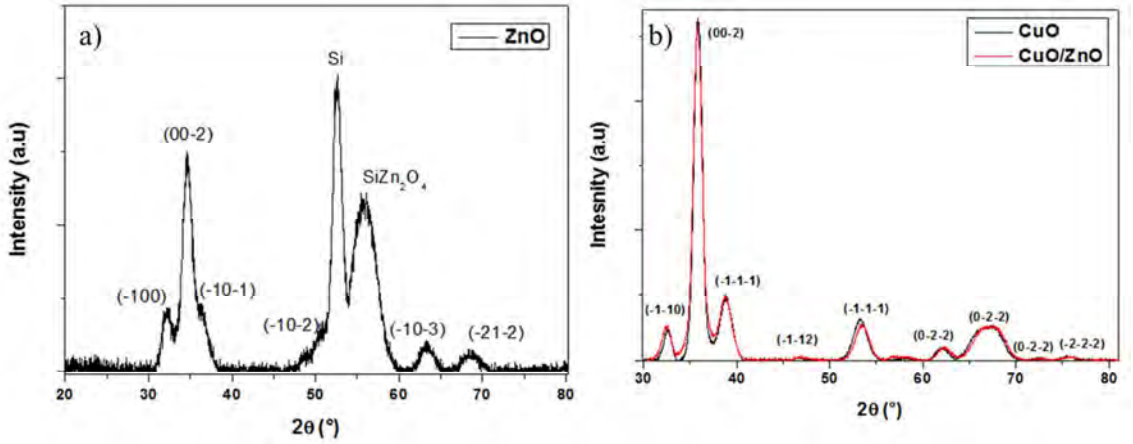

Supporting Information Figure S2. EELS spectra of oxygen between 520 and 580 eV, copper and zinc taken in the CuO layer, at 10 nm, 20 and 30 nm from the initial CuO/ZnO surface. Spectra correspond to the foils with an interfacial ZnO layer of 8 nm.

In red, at 10 nm from the initial CuO/ZnO surface, we detect only Al and oxygen. In green, at 20 nm from the initial CuO/ZnO, we detect the coexistence of CuO, Al, O and Zn. In purple, at 30 nm from the initial CuO/ZnO surface, we detect the coexistence of CuO and Zn.

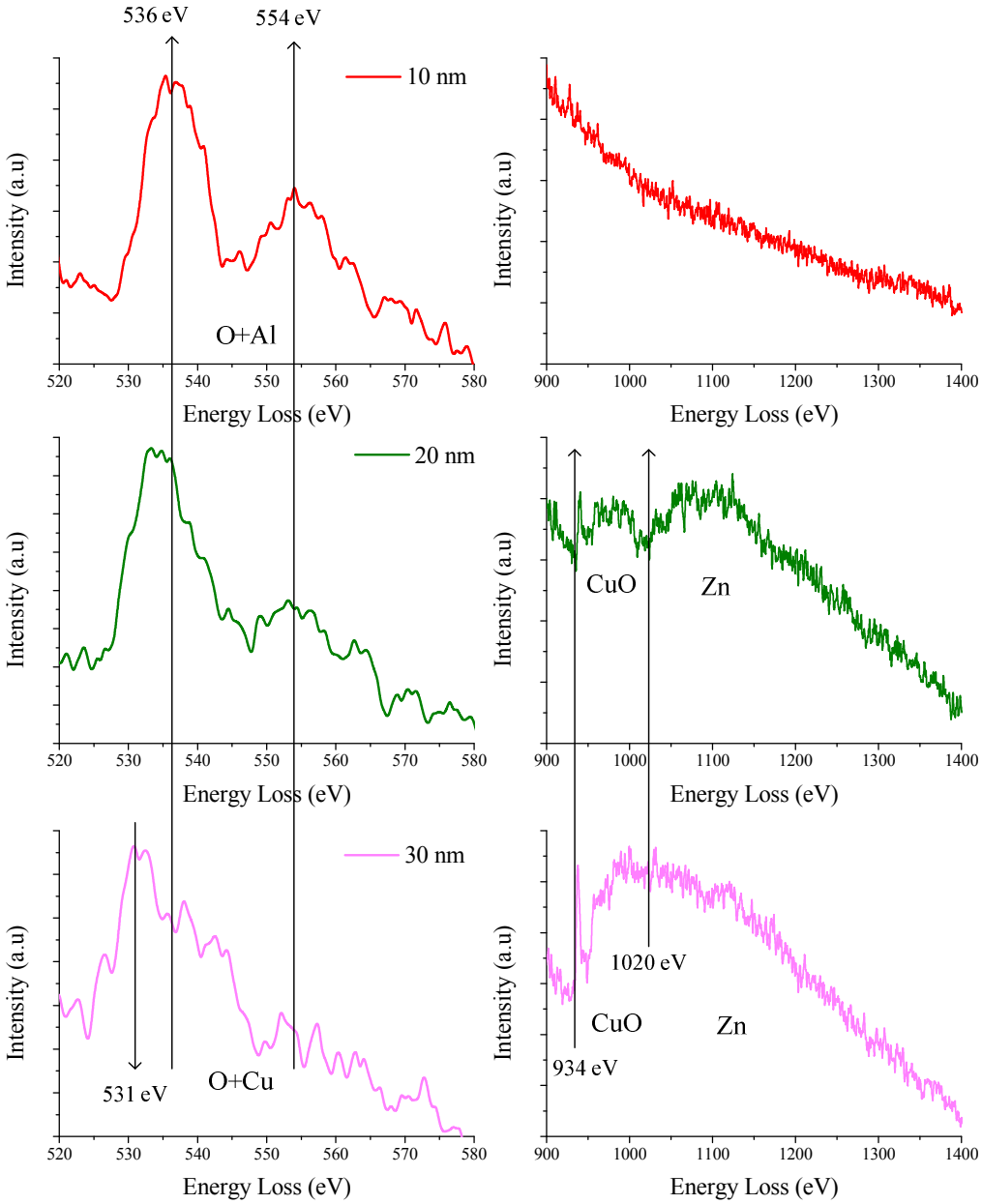

Supporting Figure S3. X-ray patterns of one CuO/Al bilayer samplewith natural interfaces (reference), CuO/ZnO/Al foil with 8 nm of ZnO as interfacial layer, and CuO/ZnO/ Al_2O_3/Al foil with 2 nm Al_2O_3 on ZnO prior the sputter deposition of Al.

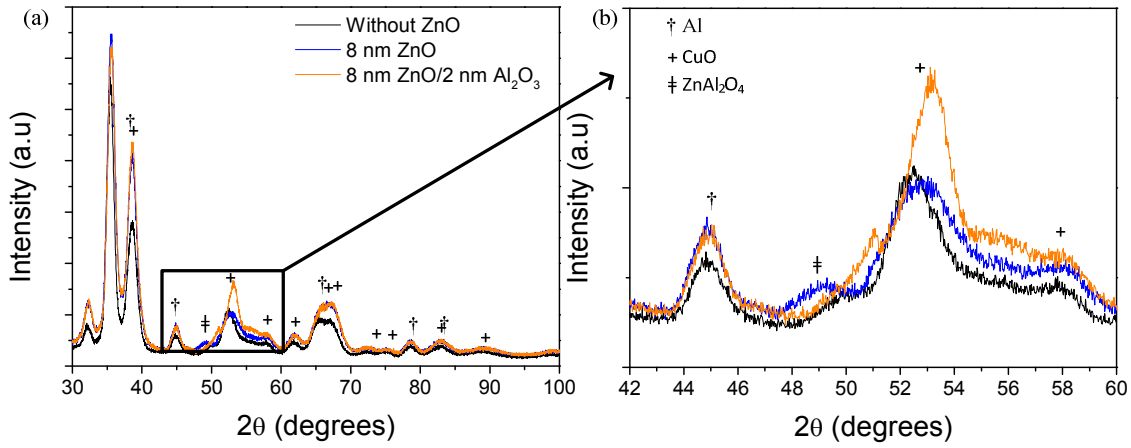

Supporting Figure S4. X-ray patterns of : *Black.* CuO/Al, *Blue.* CuO/ZnO/Al (8 nm of ZnO) and *Green.* CuO/ZnO/Al (16 nm of ZnO) as deposited (*left*) and after storage at ambient during 250 days (*right*). After 250 days, the composition of the sample without ZnO interfacial layer changes. CuO (+) and Al (†) are still the main phase but a new peak around 42.486° appears corresponding to Cu_2O. However, the composition of the samples with ZnO interfacial layer, no evolution in the composition is seen after 250 days stored at ambient. Note that, the intensity of the small peak ~ 49.062° (corresponding to $ZnAl_2O_4$) diminishes after 250 days.